

System Identification Approach Applied to Jitter Estimation.

Frans Verbeyst^{1,2}, Yves Rolain¹, Johan Schoukens¹ and Rik Pintelon¹

¹department ELEC, Vrije Universiteit Brussel, Pleinlaan 2, B-1050 Brussels, Belgium, yves.rolain@vub.ac.be

²NMDG Engineering BVBA, C. Van Kerckhovenstraat 110, B-2880 Bornem, Belgium, frans.verbeyst@nmdg.be

Abstract - A system identification approach is applied to estimate the jitter introduced by a high-frequency sampling oscilloscope. An extended model is proposed to describe the sample variance of a set of repeated (impulse response) measurements in the presence of additive and jitter noise. Then, the (weighted) least-squares and maximum likelihood estimator are introduced to estimate the standard deviation of this additive and jitter noise. First, results are shown based on simulations. These allow to test both the correctness of the implementations, to verify the ability to detect model errors and to study the effect of uncertainties on the input signal. Next, the jitter and additive noise standard deviation are estimated on real measurements by performing impulse response measurements using an Agilent 83480A sampling oscilloscope in combination with 83484A 50 GHz electrical plug-ins. Additional challenges, such as the conjugated effect of time base drift and time base distortion, are described and correctly taken care of, demonstrating the real power of a solid stochastic framework.

Keywords - time base jitter, system identification, sampling oscilloscopes, time base distortion, time base drift.

I. INTRODUCTION

Sampling oscilloscopes suffer from time base distortion, time base drift and time base jitter. Here we focus on the impact of jitter effects. Given a symmetrical probability density function, jitter does not introduce phase distortion. However, it has a low-pass effect on the amplitude characteristic [1]. As such correct jitter estimation is important, for instance, during the crossverification of the amplitude distortion of a 50 GHz sampling oscilloscope based on the nose-to-nose calibration technique [2] and the electro-optic sampling (EOS) system [3].

High-frequency sampling oscilloscopes often use an equivalent-time sampling principle and suffer from both additive measurement noise $n_y(t_i)$ and timing jitter noise $n_t(t_i)$ at the sampling time instance t_i .

$$y(t_i) = y_0(t_i + n_t(t_i)) + n_y(t_i) \quad (1)$$

$y(t_i)$ represents the measurement of the exact signal $y_0(t_i)$ when both additive noise and jitter are added as part of the measurement. Both $n_y(t_i)$ and $n_t(t_i)$ are assumed to be zero mean, normally distributed, independent and stationary with respect to t .

Recent work with respect to jitter estimation [4], [5] is based on a first order Taylor approximation of $y_0(t_i + n_t(t_i))$:

$$\tilde{y}_1(t_i) = y_0(t_i) + \left. \frac{dy_0}{dt} \right|_{t=t_i} \cdot n_t(t_i) + n_y(t_i) \quad (2)$$

Given zero mean additive and jitter noise, the expected value of $\tilde{y}_1(t_i)$ equals $y_0(t_i)$. Thus, this first order approximation cannot explain the low-pass effect introduced by jitter. Furthermore, the variance of $\tilde{y}_1(t_i)$ equals

$$\tilde{\sigma}_{y_1}^2(t_i) = \sigma_{n_y}^2 + \left. \left(\frac{dy_0}{dt} \right)^2 \right|_{t=t_i} \cdot \sigma_{n_t}^2 \quad (3)$$

σ_{n_y} and σ_{n_t} represent the standard deviation of the additive and jitter noise. Both are estimated by performing M repeated measurements $y^{[k]}(t_i)$, $k = 1, \dots, M$ of the unknown exact signal $y_0(t_i)$. Notice that according to (3), $\tilde{\sigma}_{y_1}^2(t_i)$ must equal $\sigma_{n_y}^2$ whenever $\left. \frac{dy_0}{dt} \right|_{t=t_i} = 0$. Measurements show that the latter is not true, neither for nose-to-nose nor for other high-frequency impulse response measurements, such as the impulse response of the opto-electrical (O/E) converter which was calibrated using the EOS system.

Moreover, it was found that both time base drift and time base distortion compensation shape the sample variance $\tilde{\sigma}_{y_1}^2(t_i)$ and must properly be dealt with in order to obtain a good estimate for the standard deviation of both the jitter and the additive noise. Failing to do so, measurements show that a bias of more than 10% is introduced on the estimated variance of the additive noise.

II. EXTENDED MODEL

Based on the observation that $\tilde{\sigma}_{y_1}^2(t_i)$ does not equal $\sigma_{n_y}^2$ whenever the derivative of the unknown exact signal $y_0(t_i)$ equals zero, it is decided to extend the series approximation to include also the second and third order contributions:

$$\tilde{y}_3(t_i) = y_0(t_i) + \sum_{k=1}^3 \frac{1}{k!} \cdot \left. \frac{d^k y_0}{dt^k} \right|_{t=t_i} \cdot n_t^k(t_i) + n_y(t_i) \quad (4)$$

Calculating the expected value of $\tilde{y}_3(t_i)$, one finds

$$E[\tilde{y}_3(t_i)] = y_0(t_i) + \frac{1}{2} \cdot \left. \left(\frac{d^2 y_0}{dt^2} \right)^2 \right|_{t=t_i} \cdot \sigma_{n_t}^2 \quad (5)$$

A bias now becomes apparent and approximates the low-pass effect introduced by jitter. Let $y_0(t) = A \cdot \sin \omega t$, then $E[\tilde{y}_3(t_i)] = A \cdot (1 - \omega^2 \cdot \sigma_{n_t}^2/2) \cdot \sin \omega t$.

Calculating the variance of $\tilde{y}_3(t_i)$ gives

$$\begin{aligned} \sigma_{y_3}^2(t_i) &= \sigma_{n_y}^2 + (dy_0/dt)^2 \Big|_{t=t_i} \cdot \sigma_{n_t}^2 \\ &+ [1/2 \cdot (d^2y_0/dt^2)^2 + (dy_0/dt) \cdot (d^3y_0/dt^3)] \Big|_{t=t_i} \cdot \sigma_{n_t}^4 \\ &+ 5/12 \cdot (d^3y_0/dt^3)^2 \Big|_{t=t_i} \cdot \sigma_{n_t}^6 \end{aligned} \quad (6)$$

Based on (6), $\sigma_{y_3}^2(t_i)$ is now larger than $\sigma_{n_y}^2$ when $dy_0/dt \Big|_{t=t_i}$ equals zero, unless the second and third derivatives are also both zero.

III. ESTIMATORS

The goal is to estimate σ_{n_y} and σ_{n_t} .

A. Linear and nonlinear least squares

Starting from N independent and identically distributed (i.i.d.) measurements, one minimizes the following cost with respect to the unknown variances $\sigma_{n_y}^2$ and $\sigma_{n_t}^2$:

$$V_{LS} = \sum_{i=1}^N e^2(t_i), \quad (7)$$

$$e(t_i) = \left[\sigma_{t_i}^2 - \tilde{\sigma}_y^2(t_i, \theta) \right] / W_i. \quad (8)$$

$\sigma_{t_i}^2$ corresponds to the measured sample variance for $t = t_i$, while $\tilde{\sigma}_y^2(t_i, \theta)$ represents the model of the noise variance with $\theta = [\sigma_{n_y}^2, \sigma_{n_t}^2]^T$ and W_i is the optional weighting.

For the unweighted least squares (LS), W_i is set to 1, while the square root of the sample variance of $\sigma_{t_i}^2$ is used for the weighted least squares (WLS).

Using the first order model (3) for the noise variance, the error $e(t_i)$ is linear in the unknowns $\sigma_{n_y}^2$ and $\sigma_{n_t}^2$. However, if the model is expanded towards a higher order Taylor approximation (6), the problem is no longer linear in $\sigma_{n_t}^2$.

B. Maximum Likelihood (ML) estimator

In [4] it is shown that the ML estimator of model (3) produces statistically more efficient estimates for $\sigma_{n_y}^2(t_i)$ and $\sigma_{n_t}^2(t_i)$ than a linear least squares estimator.

This estimator uses the knowledge that, if each stochastic variable X_i has a $N(0, 1)$ normal distribution with unity variance and zero mean, then $\sum_{i=1}^r X_i^2$ has a χ_r^2 chi-squared distribution with r degrees of freedom. If the mean value of X_i is unknown, the (sample) mean has to be calculated and the number of degrees of freedom has to be decreased by 1.

It can be shown that, based on N i.i.d. measurements, the ML estimator minimizes the cost

$$V_{ML} = n/2 \cdot \sum_{i=1}^N \left[\ln \tilde{\sigma}_y^2(t_i, \theta) + \sigma_{t_i}^2 / \tilde{\sigma}_y^2(t_i, \theta) \right] \quad (9)$$

with respect to $\sigma_{n_y}^2$ and $\sigma_{n_t}^2$, where n represents the number of degrees of freedom. Performing M repeated measurements $y^{[k]}(t_i)$, $k = 1, \dots, M$ of the unknown exact signal $y_0(t_i)$ and using both sample mean and sample variance, n equals $M - 1$.

Also, it is straightforward to extend the above ML cost to deal with situations where the number of degrees of freedom varies with i . The relevance of this extension will become clear below, when dealing with time base drift.

IV. SIMULATION RESULTS

First the different models and estimators are tested using simulation data.

A. Generation of simulation data

This data is kept as realistic as possible. Therefore, the combined impulse response of a real-world opto-electrical converter (O/E) and a 50 GHz sampling oscilloscope is used as a starting point. Fig. 1 shows the block diagram of the required setup. The second O/E in the trigger path is solely used to convert the optical pulse into an electrical pulse that can be used to trigger the sampling oscilloscope.

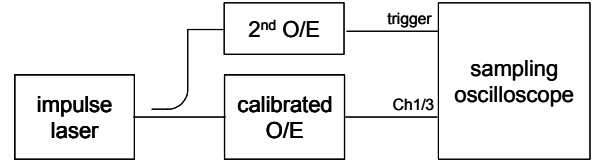


Fig. 1. Block diagram of the setup used during the impulse measurement.

During the measurement of the impulse response, 500 time records of 5 ns (4096 points each) are acquired. The data is corrected for time base drift and time base distortion.

Fig. 2 zooms in to the main portion of the averaged pulse and its corresponding sample variance. It is clearly shown that at the time instants where the averaged pulse has a zero slope, the variance is larger than the constant level at both sides of the pulse, which corresponds to the variance of the additive noise. This means that (3) does not correspond to the exact model for the measured jittered signal.

After applying a window in both the frequency and the time domain, the resulting analytical expression for the time signal is given by its Fourier series

$$x(t) = Re \left(\sum_{h=0}^H X(h) \cdot e^{j2\pi h \cdot \Delta f \cdot t} \right) \quad (10)$$

and allows to calculate the exact derivatives. $Re(x)$ represents the real part of the complex value x . If the number of relevant spectral lines H becomes too large, the calculation

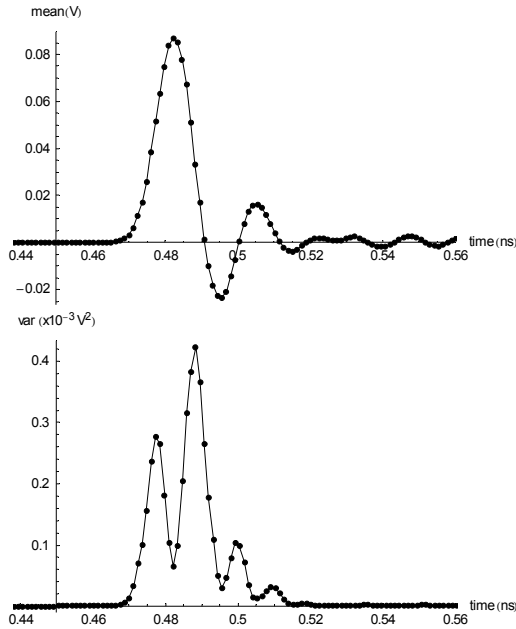


Fig. 2. Zooming into the main portion of the averaged impulse response and its variance.

of $x(t)$ using (10) becomes very time consuming and a fast inverse Fourier transform is used instead. However, when simulating jitter noise, the time samples are no longer on an equidistant grid. In order to avoid the calculation using (10), a two step approach is used. First, $x(t)$ is evaluated on a sufficiently oversampled equidistant time grid. Then, cubic interpolation is used to obtain the value at $x(t+n_t(t))$ [8]. Given the above impulse response, it was found that oversampling by a factor of 128 in combination with cubic interpolation leads to an RMS value for the difference between the exact and interpolated signal that is about 200 dB down with respect to the RMS value of the signal.

B. Third order approx. of variance, known derivatives

In order to test the correctness of the model parameter extraction software, simulation data is generated using (6). The required derivatives are based on (10) and are assumed to be known exactly. Based on measurements using the Agilent 83480A Digital Communications Analyzer, the standard deviation of the additive noise during the simulations was set to 0.6 mV, while the jitter standard deviation was stepped from 0 to 2 ps in 0.2 ps steps.

The simulation results show that the estimated parameters converge to the exact parameters when no model errors are present. It is also verified that the uncertainty on the parameters, indicated by the parameter covariance matrix, corresponds to the sample variance of the parameters based on repeated estimations.

In case of the WLS estimator, it is found that both the sample mean and sample variance of the cost match their expected value within their 95% confidence intervals when there are no model errors (3rd order model), while there is a

significant difference when there are model errors (1st and 2nd order model) for increasing values of the jitter standard deviation (Fig. 3). This clearly shows the capability of the WLS estimator with respect to model selection.

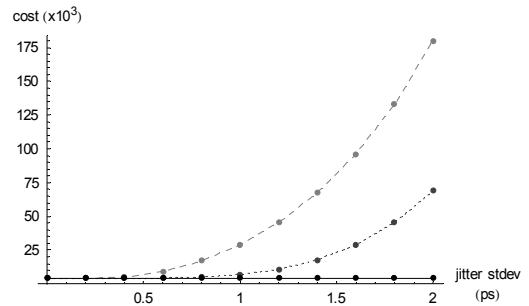


Fig. 3. Mean value of the cost using the WLS estimator. (1st order model: long dashed line, 2nd order model: short dashed line, 3rd order model: solid line, expected value of cost: 4136)

C. Realistic variance, known and unknown derivatives

Next, more realistic simulations are performed using “real” jitter, starting from (1). The simulations also allow to study the effect of uncertainties on the input signal. More specifically, first the exact derivatives of the exact signal are used, while in a next step, these derivatives are calculated from the measured data using the sample mean of the signal. It was found that the effect of not knowing the exact derivatives is negligible.

The simulation results show that the unweighted LS estimator provides the best estimates for the jitter standard deviation, while the WLS estimator outperforms the LS when estimating the standard deviation of the additive noise. This is due to the presence of model errors and the fact that the jitter has a larger contribution to the LS cost than to the WLS cost.

Using a third order model in combination with the WLS estimator, Fig. 4 clearly shows that the sample mean of the cost and its 95% confidence interval include the expected value of the cost for jitter standard deviation values up to 1 ps. For higher jitter values, the sample mean of the cost clearly starts to deviate from the expected value indicating the presence of model errors.

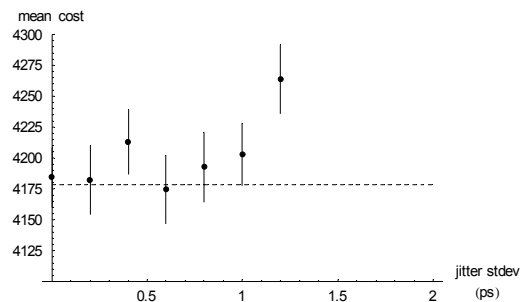


Fig. 4. Expected value (dashed line) of the cost of the 3rd order model using the WLS estimator, compared to its sample mean value (50 realizations) and its 95% confidence interval. The mean cost for jitter standard deviations of more than 1.2 ps fall outside the selected vertical range.

D. Conclusions and guidelines

The WLS estimator provides model selection capability. In the absence of model errors, both the ML and WLS estimator are preferred because they provide more efficient estimates than the LS estimator. In the case of model errors ($\sigma_{n_i} > 1$ ps), the LS estimator provides better estimates for the jitter standard deviation, while the ML and WLS estimator do a better job in estimating the standard deviation of the additive noise.

V. INFLUENCE OF TIME BASE DRIFT

The above simulations show that all estimators perform reasonably well when the jitter standard deviation is limited to 1 ps. Applying them to measured data, large discrepancies were found between the measured and estimated variance, even though the estimated jitter standard deviation also turns out to be about 1 ps. The sampling oscilloscope measurements add extra challenges due to time base drift and time base distortion, which were not included in the simulations. As such, it is decided to study the effect of time base drift and its compensation on the estimated parameters.

A. Theory

Let $x_n = x(n \cdot \Delta t)$ represent the sampled version of a band limited signal $x(t)$. It is possible to write the sampled version of the delayed signal $x'(t) = x(t - \tau)$ as

$$x'_n = x'(n \cdot \Delta t) = \sum_{k=-\infty}^{+\infty} x_k \cdot \text{sinc}[\pi(n - k - \tau/\Delta t)] \quad (11)$$

(11) clearly shows that for an arbitrary delay τ , x'_n depends on all x_k and is no longer independent with respect to n . However, if $\tau = m \cdot \Delta t$, all contributions are zero, except for $k = n - m$. Thus, $x'_n = x_{n-m}$. As such, unless the applied delay is an integer multiple of the sampling period, the variance of the delayed signal does not equal the variance of the original signal. In this article, this effect is referred to as the shaping of the variance due to time base drift compensation.

B. Simulation

The analytical pulse (10) is used to study the shaping of the variance as function of $\tau/\Delta t$. First a known delay $\tau = k \cdot \Delta t/10$, $k = 1 \dots 5$, $\Delta t = 5/4096$ ns is applied to the analytical pulse. The sample variance of this delayed pulse is obtained based on 1000 realizations using a standard deviation of 0.6 mV of the additive noise and a standard deviation of 1 ps of the jitter noise. Next the inverse delay is applied to this sample variance and compared to the sample variance of the original pulse. Fig. 5 shows the difference between the original variance and the variance after delay compensation of $0.5\Delta t$. If the delay is limited to $0.1\Delta t$, it is found that the resulting shaping is negligible.

C. Reducing the shaping of the variance

In order to limit the error introduced by time base drift

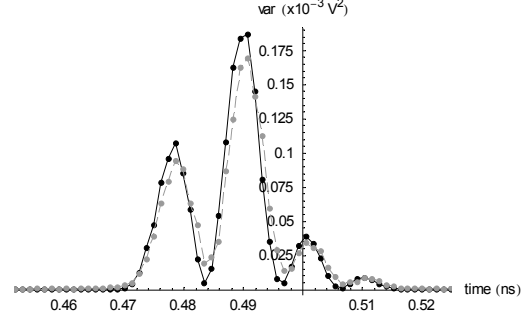


Fig. 5. Clear shaping of the sample variance (solid black line: original variance, dashed gray line: variance after delay compensation of $0.5\Delta t$)

compensation before averaging, the different realizations of the pulse are first delayed by integer multiples of Δt such that all realizations are aligned within $\pm 0.5\Delta t$. Then all realizations are divided into time buckets which are $\pm 0.1\Delta t$ wide, resulting in a 5-times oversampled signal compared to the original signal. Further processing of this oversampled signal is explained in the following section.

VI. MEASUREMENT RESULTS

The measurement data correspond to the combined impulse response of an opto-electrical converter and a 50 GHz sampling oscilloscope (see Fig. 1). A time record of 5 ns was used starting at 143 ns delay and 5000 records of 4096 points were acquired. Each measurement takes about 0.45 seconds.

A. Time base drift estimation

The drift is estimated, using the first measurement as reference and by minimizing

$$V_{TBDt} = \sum_{i=1}^N \left| X_{ref}(\omega_i) - e^{-j\omega_i \tau} \cdot X(\omega_i) \right|^2 \quad (12)$$

within the bandwidth of the signal $X(\omega_i)$. Based on the fact that simulations confirmed that time base jitter may incorrectly be interpreted as time base drift and based on reasonable time constants corresponding to thermal effects, which are assumed to cause the time base drift, the estimated drift is smoothed.

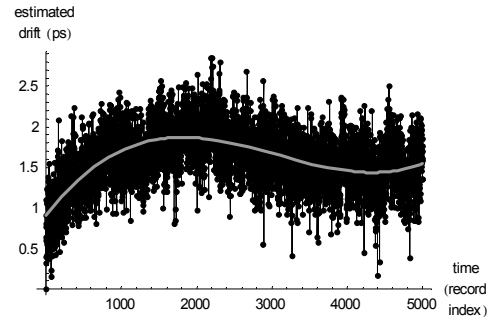


Fig. 6. Estimated time base drift (gray: smoothed using 4th order polynomial)

B. Time base drift compensation

The smoothed version of the estimated time base drift, based on a 4th order polynomial, is used to align the different

realizations. First all realizations are aligned within $\pm 0.5\Delta t$. This does not introduce any shaping of the variance, as only shifts over an integer number of samples are used. Next, the realizations are divided in 5 buckets, each being $\pm 0.1\Delta t$ wide. All realizations within each bucket are aligned with respect to the center of that bucket. Given a maximum delay of $0.1\Delta t$, the resulting shaping of the variance that is introduced by this alignment can be neglected. Fig. 7 shows the unequal distribution of the 5000 realizations over the different buckets.

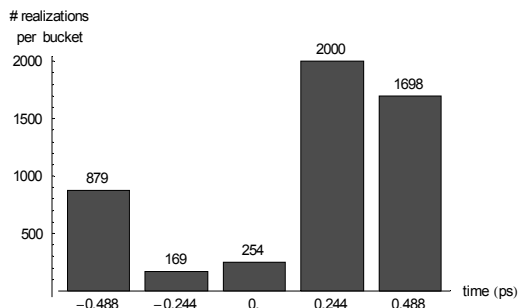


Fig. 7. Distribution of the 5000 realizations over the different buckets.

In order to obtain variance information, required by the WLS estimator, different approaches are possible. First, one can divide the realizations into different data sets. The effect of using the sample variance, instead of the exact variance, on the expected value and variance of the cost and on the uncertainty of the parameters as function of the number of the data sets, is studied in [6]. Another option is to use the knowledge that, for a sufficiently large number of realizations, the variance of the sample variance of the pulse is χ^2 -distributed. Both approaches result in estimates for the standard deviation of the additive and jitter noise which match within their 95% confidence intervals.

C. Time base distortion estimation and compensation

Due to the time base distortion of the Agilent 83480A Digital Communication Analyzer, the sample mean and the sample variance are specified on a non-equidistant time grid. The time jitter estimation algorithm used in this article does not require the sample mean and sample variance to be specified on an equidistant time grid. However, in order to efficiently calculate the derivatives of the mean pulse via the frequency domain using an FFT, cubic interpolation is used to obtain the values of the sample mean on an equidistant grid, as proposed in [8]. The derivatives are obtained at the original non-equidistant grid by applying the “inverse” cubic interpolation. The time base distortion is estimated using [7], after collecting the required data.

D. Time base jitter estimation

Finally, the time base jitter can be estimated using the proposed model (6) and the weighted least squares estimator, taking the varying variance of the sample variance as function of the bucket index into account, in order to minimize the

uncertainty on the estimated parameters. Fig. 8 shows the measured variance on a logarithmic scale, after proper compensation of the time base drift. Fig. 9 horizontally zooms into the jitter portion and compares the modelled variance (6) to the measured variance and its 95% confidence interval based on a χ^2 -distribution. Fig. 10 vertically zooms into the additive noise portion.

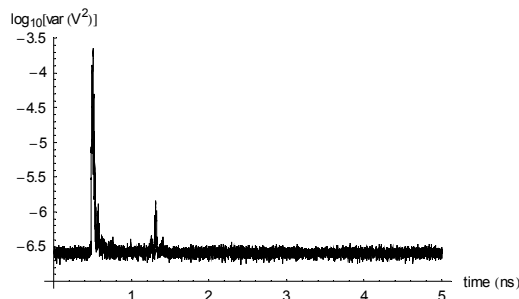


Fig. 8. Correctly aligned “measured” variance (logarithmic vertical scale).

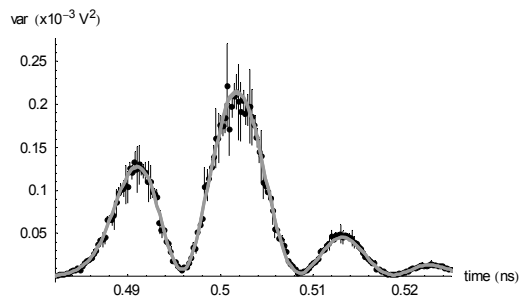


Fig. 9. Comparing the modelled (gray) and correctly aligned “measured” variance (black dots and vertical lines corresponding to 95% confidence intervals based on the χ^2 -distribution of its sample variance). Zooming horizontally into the jitter portion of the variance.

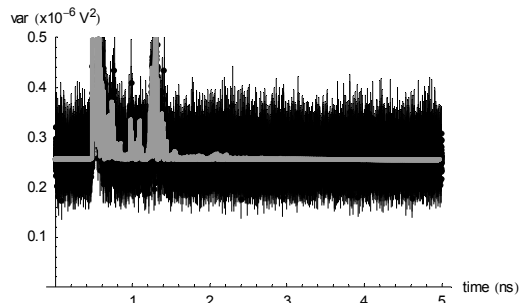


Fig. 10. Comparing the modelled (gray) and correctly aligned “measured” variance (black dots and vertical lines corresponding to 95% confidence intervals based on the χ^2 -distribution of its sample variance). Zooming vertically into the additive noise portion of the variance.

The value of the WLS cost function turns out to be 7% larger than the expected value of the cost and is located slightly outside the 95% confidence interval of the expected value of the cost. The standard deviation of the estimated additive and jitter noise and their 95% confidence intervals are $0.508 \text{ mV} \pm 0.16 \text{ }\mu\text{V}$ and $0.965 \text{ ps} \pm 2.3 \text{ fs}$.

Excellent correspondence was found between the

estimated standard variation of both jitter and additive noise, based on the LS estimator, the WLS estimator and the ML estimator. The WLS estimator is to be preferred because the actual value of the cost can be used to detect model errors by comparing it to its expected value, while this is impossible for the LS estimator. Furthermore, the uncertainty on both estimated parameters is significantly smaller using the WLS and ML estimator. Interpreting the value of the cost based on the ML estimator is found to be less obvious. Also the χ^2 distribution used for the MLE is only 100% valid for the first order model.

E. The power of a stochastic framework

Suppose the shaping of the variance due to time base drift compensation is overlooked. Repeating the estimation procedure, the expected value of the cost and its 95% confidence interval equals 4212 ± 188 . The realized cost using a third order model turns out to be 14764, which is 3.5 times the expected value of the cost. As can be seen in Fig. 11, this is confirmed by a poor fit when the variance to be modelled is based on incorrectly processed measurements.

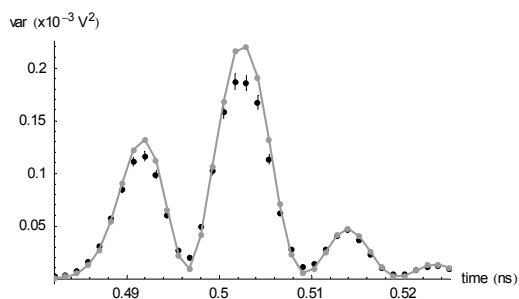


Fig. 11. Comparing modelled (gray) and incorrectly shaped “measured” variance (black dots and vertical lines corresponding to 95% conf. interval).

F. Bias in estimation of variance of additive noise

Finally, it is mentioned that overlooking the shaping of the variance, due to time base drift compensation, in combination with the first order model and the LS estimator, introduces a bias of more than 10% on the estimated variance of the additive noise. This may explain why in [5] the additive noise is estimated separately. It is found that this offset is removed by properly aligning the pulses, as proposed in this article.

VII. CONCLUSIONS

The system identification approach described in this article and applied to jitter estimation of the combined impulse response of an opto-electrical converter and a high-speed sampling oscilloscope is a major extension of [4], which can be applied to “real” problems. Indeed, the simulation results presented in [4] are based on the rather unrealistic assumption that (3) is the exact representation of the sample variance, while in reality it is only a first order approximation.

The underlying stochastic framework allows to detect

model errors and anomalies like the shaping of the variance due to time base drift compensation. Error bounds are provided on both the estimated parameters and the modelled variance. Finally, the method allows the simultaneous estimation of the variance of the additive noise and the jitter noise, where other methods [5] fail to do so.

VIII. ACKNOWLEDGEMENT

The impulse response measurement and the required time base distortion measurements were performed by Tracy Clement of the Optoelectronics Division at NIST in Boulder. This contribution is gratefully acknowledged by the authors.

Part of this work is sponsored by the Fund for Scientific Research (FWO-Vlaanderen), the Flemish Government (GOA-Illinois) and the Belgian Program on Interuniversity Poles of Attraction initiated by the Belgian State, Prime Minister’s Office, Science Policy programming (IUAP V/22).

Research reported here is also performed in the context of the network TARGET – “Top Amplifier Research Groups in a European Team” and supported by the Information Society Technologies Programme of the EU under contract IST-1-507893-NOE, www.target-net.org.

IX. REFERENCES

- [1] T. Souders, D. Flach, C. Hagwood and G. Yang, “The Effects of Timing Jitter in Sampling Systems,” *IEEE Transactions on Instrumentation and Measurement*, Vol. 39, No. 1, February 1990
- [2] P. Hale, T. Clement, K. Coakley, C. Wand, D. DeGroot and A. Verdoni, “Estimating the Magnitude and Phase Response of a 50 GHz Sampling Oscilloscope Using the “Nose-To-Nose” Method,” *55th ARFTG Conf. Digest*, June 2000
- [3] D. Williams, P. Hale, T. Clement and J. Morgan, “Calibrating electro-optic sampling systems,” *Int. Microwave Symposium Digest*, Phoenix, AZ, pp. 1527-1530, May 20-25, 2001
- [4] G. Vandersteen and R. Pintelon, “Maximum Likelihood Estimator for Jitter Noise Models,” *IEEE Transactions on Instrumentation and Measurement*, Vol. 49, No. 6, December 2000
- [5] K. Coakley, C.-M. Wang, P. Hale and T. Clement, “Adaptive Characterization of Jitter Noise in Sampled High-Speed Signals,” *IEEE Transactions on Instrumentation and Measurement*, Vol. 52, No. 5, October 2003
- [6] J. Schoukens, R. Pintelon and Y. Rolain, “Maximum Likelihood Estimation of Errors-In-Variables Models using the Sample Covariance Matrix Obtained from Small Data Sets,” published as part of “*Recent Advances in Total Least Squares Techniques and Errors-In-Variables Modeling*”, Sabine Van Huffel (editor), Siam, Philadelphia, 1997
- [7] G. Vandersteen, Y. Rolain and J. Schoukens, “An Identification Technique for Data Acquisition Characterization in the Presence of Nonlinear Distortions and Time Base Distortions,” *IEEE Transactions on Instrumentation and Measurement*, Vol. 50, No. 5, October 2001
- [8] Y. Rolain, J. Schoukens and G. Vandersteen, “Signal Reconstruction for Non-Equidistant Finite Length Sample Sets: a “KIS” approach,” *IEEE Transactions on Instrumentation and Measurement*, Vol. 47, No. 5, October 1998, pp. 1046 - 1052